Design and simulation of an integrated optical circulator on InP membrane platform

Rui Ma*, Sander Reniers, Zizheng Cao, Kevin Williams, Yuqing Jiao, Jos van der Tol

Institute for Photonic Integration (IPI), Eindhoven University of Technology, PO Box 513, 5600 MB Eindhoven, The Netherlands

* r.ma@tue.nl

A 4-port optical circulator on an InP membrane platform is proposed. The circulator is composed of two multi-mode interference couplers (MMIs), four polarization converters (PCs) and a cerium-doped yttrium iron garnet (Ce: YIG) layer. The Ce: YIG layer is bonded on top of the InP waveguides. Non-reciprocal phase shift (NRPS) will be employed when an external magnetic field is applied to the Ce: YIG layer. The circulator design predicts a maximum isolation of 41.1 dB, crosstalk of 41.2 dB and insertion loss of 1.7 dB at a wavelength of 1550 nm in simulation.

Introduction

In InP membrane platform, a thin InP membrane is adhesively bonded to a silicon wafer using benzocyclobutene (BCB) polymer. The high contrast obtained in this way makes the platform suitable for high-density photonic integrated circuits (PICs). Many kinds of optical active and passive devices have been investigated in the InP membrane platform [1], such as DBR lasers, SOAs, MMIs, grating couplers, and PCs. To achieve a highly functional PIC, optical circulators are highly desired. For example, optical circulators are indispensable in the wavelength-division multiplexing system and optical coherence tomography system. However, current commercial bulky circulators are added on the module level, which implies a significant proportion of the PIC package cost.

Recently, several integrated optical circulators based on different platforms have been demonstrated. In 2013, Kota [2] et al fabricated a 4-port silicon waveguide optical circulator employing a Mach–Zehnder interferometer (MZI) configuration. The circulator operation was demonstrated with a maximum isolation of 15.3 dB at a wavelength of 1531 nm. In 2013, Samir et al [3] demonstrated a 3-port optical circulator on the silicon-on-insulator (SOI) platform and an isolation of 22 dB was measured at a wavelength of 1562 nm. In 2017, Huang et al [4] demonstrated 4- and 6-port optical circulators utilizing a silicon micro-ring-resonator with a bonded magneto-optic cladding alongside an integrated electromagnet. The measured isolation is up to 14.4 dB at a wavelength of 1558 nm. However, these designs could only work for TM mode input, because Ce: YIG is bonded on top of the structure and only the TM mode experiences the non-reciprocal interaction with the Ce: YIG layer.

In this paper, we demonstrate a 4-port optical integrated circulator based on an InP membrane platform. An advantage of this device is its compatibility with both TE and TM-mode inputs.

Device design

The device is designed based on the InP membrane on silicon (IMOS) platform. A schematic of the device is shown in Fig. 1. The circulator is based on a Mach-Zehnder interferometer, including two MMIs, four polarization converters [5] and a Ce: YIG layer.

For the polarization converter, two triangular waveguides and one rectangular waveguide section are used. The slanted wall of the triangular waveguide can be obtained by wet etching at an angle of 35° with respect to the (001) plane. The polarization converter can realize TE-TM polarization conversion due to its geometry. The Ce: YIG layer is bonded as an upper-cladding material on top of the InP waveguides. A non-reciprocal phase shift (NRPS) effect will be present when an external magnetic field is applied [6].

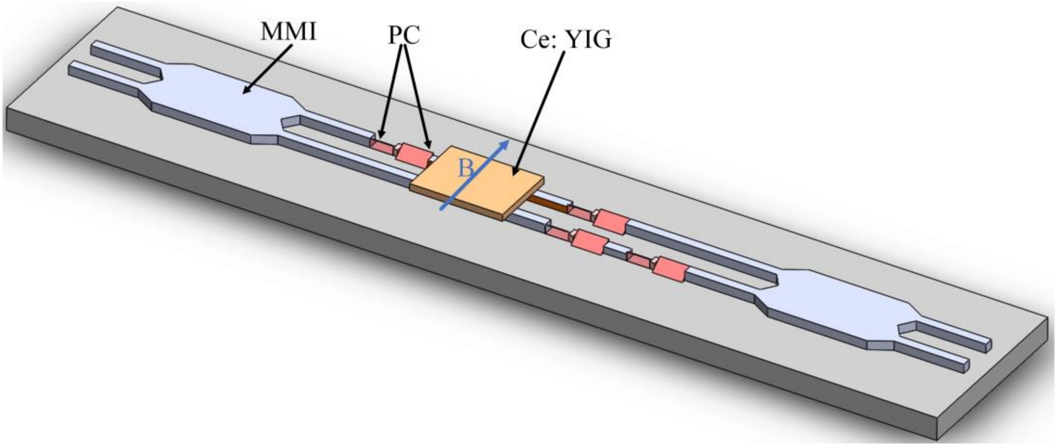

Fig. 1 Schematic of the circulator

Operation Principle

The schematic configuration is shown in Fig. 2. As shown in Fig. 2(a), for the forward direction, the input signal coupled into port 1 is split into two branches by MMI 1. The signals in both arms have equal power but a phase difference of π/2. If the input is TE mode, it will be converted to TM mode after passing through PC 1 in the upper branch. Then, part of the TM mode will propagate in the Ce: YIG layer, which will provide a non-reciprocal phase shift. The TM mode will be converted back to TE mode after PC 2. In the lower branch, the TE mode will not be affected by NRPS effect. The TE mode signal in the lower branch will be converted to TM mode after PC 3 and be converted back to TE mode after PC 4. PC 3 and PC 4 are used to balance the losses in the two branches. Furthermore, the birefringence in the waveguides will cause a reciprocal phase shift (RPS) between the signals in the two branches.

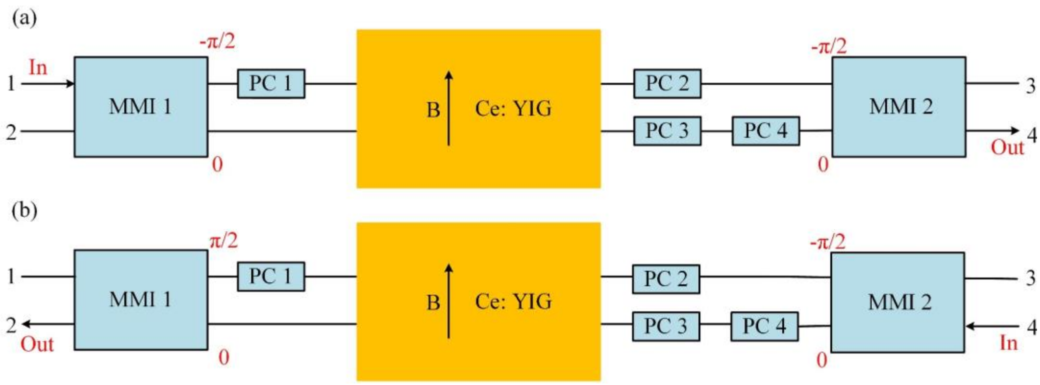

Fig. 2 Schematic diagram of the circulator (a) Forward direction (b) Backward direction

If the input signal is TE mode, the phase differences for the forward and backward directions can be written as:

$$(\beta_{TE,RPS} - \beta_{TM,RPS}) \cdot L_1 - \beta_{TM,NRPS_F} \cdot L_2 = 2n\pi \quad (1)$$

$$(\beta_{TE,RPS} - \beta_{TM,RPS}) \cdot L_1 - \beta_{TM,NRPS_B} \cdot L_2 = 2(m+1)\pi \quad (2)$$

where n and m are both integers. $\beta_{TE,RPS}$ is the propagation constant of TE mode. $\beta_{TM,NRPS_F}$ and $\beta_{TM,NRPS_B}$ are the propagation constant of the TM mode in forward and backward directions, respectively. L_1 is the length of normal waveguide. L_2 is the length of Ce: YIG layer. m and n are integers.

Thus, when both signals are combined in the output MMI, phase differences due to NRPS and RPS should be cancelled. Then the output signal will emerge in port 4. As shown in Fig. 2(b), for the backward direction, the input signal launched in port 4 will emerge from port 2 due to the π phase difference between the two branches, which is in this direction the sum of the NRPS and the RPS. The device also works on the same principle if the input signal is TM mode.

Simulation results

The proposed design in Fig. 2 is simulated in Lumerical FDTD. The length of Ce: YIG is scanned from 0 to 1 mm, in steps of 0.05 mm.

The simulation results for an input of TE-polarized light at 1550 nm are shown in Fig. 3. The vertical axis is the normalized output power distribution in the proposed device as illustrated in Fig. 2. The horizontal axis is the length of Ce: YIG. Fig. 3(a) shows the normalized output power distribution in port 3 and port 4 for forward direction [Fig. 2(a)]. Fig. 3(b) shows the normalized output power distribution in port 1 and port 2 for backward direction [Fig. 2(b)].

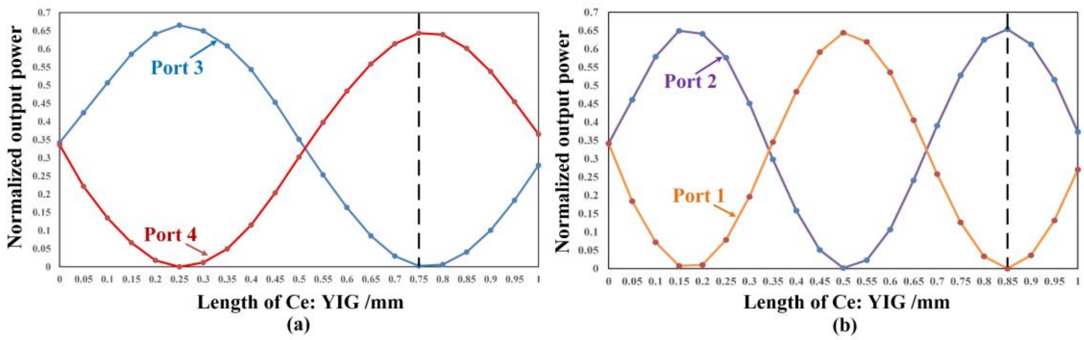

Fig. 3 Normalized output power distribution as a function of the length of Ce: YIG, for a TE polarized input signal. (a) In forward direction with input at port 1 (b) In backward direction with input at port 4

In Fig. 3, the normalized output power distribution in the two output ports is periodically varying with the length of Ce: YIG. The periods for forward and backward directions are different, because of the NRPS effect as illustrated in equation (1) and (2).

In Fig. 3(a), when the length of Ce: YIG is 0.75 mm, the TE mode signal entered from port 1 will mostly pass through port 4 in the forward direction. The crosstalk is 40.1 dB between port 3 and port 4.The insertion loss is 1.7 dB. In Fig. 3(b), when the length of Ce: YIG is 0.85 mm, the TE mode signal entered from port 4 will mostly pass through port 2 in the backward direction. The crosstalk can be obtained is 41.2 dB between port

1 and port 2.The insertion loss is 1.8 dB. The reason that the crosstalk and insertion loss are slightly different for forward and backward direction is that the splitting ratio of MMIs is not exactly 3 dB in simulation. The insertion loss mainly originates from MMIs, the interfaces between PCs, waveguide and Ce: YIG layer.

As shown in equation (1) and (2), m and n are dependent on L_1 and L_2. As mentioned above, in our simulation, n becomes an integer when the length of Ce: YIG is 0.75 mm. m becomes an integer when the length of Ce: YIG is 0.85 mm. As shown in Fig. 3, we cannot find a certain length of Ce: YIG that can make n and m both integers. There are two possible ways to fix it. First option is inserting an additional phase shifter, which will change the length of L_2. At one point, n and m could both be integers. Second option is elongating the Ce: YIG layer. Because it can be calculated that the periods of forward direction and of backward direction are 1.0 mm and 0.7 mm, respectively. In our simulation, the InP waveguide and Ce: YIG are lossless. So, the optimal length of Ce: YIG is 5.75 mm to get the best performance in forward and backward direction simultaneously. The predicted isolation of the circulator is 41.1 dB in the optimal length of Ce: YIG.

Conclusion

In this paper, a Mach-Zehnder interferometer-based four-port optical circulator for an InP membrane platform is demonstrated and simulated. The device consists of two MMIs, four PCs and a layer of Ce: YIG on top and makes use of non-reciprocal phase shift effect. The performance of circulator is predicted in simulations with a crosstalk of 41.2 dB, a minimum insertion loss of 1.7 dB and a maximum isolation of 41.1 dB at a wavelength of 1550 nm. This design can be integrated with other photonic components, like lasers and amplifiers, on the IMOS platform. Thus, it can provide a step forward towards a fully functional PIC.

References

[1] Jos van der Tol, Yuqing Jiao, Longfei Shen, et al. "Indium phosphide integrated photonics in membranes." IEEE Journal of Selected Topics in Quantum Electronics 24, 1-9 (2018).

[2] Mitsuya, Kota, Y. Shoji, and T. Mizumoto. "Demonstration of a Silicon Waveguide Optical Circulator." IEEE Photonics Technology Letters 25, 721-723 (2013).

[3] Samir Ghosh, Shahram Keyvaninia, Wim Van Roy, et al. "Adhesively bonded Ce:YIG/SOI integrated optical circulator." Optics Letters 38, 965-967 (2013).

[4] Duanni Huang, Paolo Pintus, Chong Zhang, et al. "Dynamically reconfigurable integrated optical circulators." Optica 4, 23-30 (2017).

[5] Josselin Pello, Jos van der Tol, Shahram Keyvaninia, et al., "High-efficiency ultrasmall polarization converter in InP membrane," Opt. Lett. 37, 3711-3713 (2012).

[6] Bethanie J. H. Stadler, Tetsuya Mizumoto. "Integrated Magneto-Optical Materials and Isolators: A Review." IEEE Photonics Journal 6, 1-15 (2014).